15 Erosion–Corrosion in Single and Multiphase Flow

J. POSTLETHWAITE

Department of Chemical Engineering
University of Saskatchewan, Saskatoon
Saskatchewan, Canada

S. NESIC

Department of Mechanical Engineering
University of Queensland, Brisbane
Queensland, Australia

A. INTRODUCTION

Erosion–corrosion encompasses a wide range of flow-induced corrosion processes. Flowing fluids can damage protective films on metals resulting in greatly accelerated corrosion. Damage to the films may be the result of mechanical forces or flow-enhanced dissolution and the accelerated corrosion may be accompanied by erosion of the underlying metal. This conjoint action of erosion and corrosion is known as erosion–corrosion [1]. Impingement attack by liquid droplets and solid particles, and cavitation attack are also included here, under this broad definition of erosion–corrosion. In practice, the relative contributions of *accelerated corrosion* and erosion, to the total metal loss, vary widely with the type of erosion–corrosion and the hydrodynamic intensity of the flow.

B. FLOW CONDITIONS

Erosion–corrosion normally occurs under *turbulent flow* conditions. The flowing fluid may be single phase (Fig. 1) as in the erosion–corrosion of copper tubing by potable water (Fig. 2). Multiphase flows [2–4] (Fig. 3) with various combinations of gas, water, oil, and sand can cause severe erosion–corrosion of oil/gas production systems [5–7] as shown in Figures 4–6.

The most severe erosion–corrosion problems occur under conditions of *disturbed* turbulent flow [8, 9] at sudden changes in the flow system geometry, such as bends, heat-exchanger-tube inlets, orifice plates, valves, fittings, and in turbo-machinery including pumps, compressors, turbines, and propellers. Surface defects in the form of small protrusions or depressions such as corrosion pits, deposits, and weld beads can give rise to disturbed flow on a smaller scale but sufficient to initiate erosion–corrosion [10, 11]. The presence of suspended solid particles, gas bubbles, or vapor bubbles in aqueous flow, and liquid droplets in high-speed gas flow can be especially damaging.

Uhlig's Corrosion Handbook, Second Edition, Edited by R. Winston Revie.
ISBN 0-471-15777-5

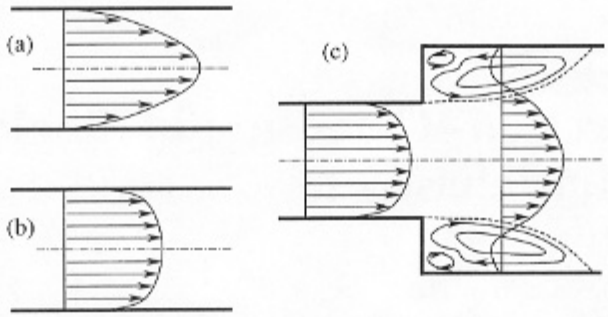

FIGURE 1. Single-phase pipe flow. (a) Developed laminar flow, showing parabolic velocity profile. (b) Developed turbulent flow, showing logarithmic velocity profile with large gradients near the wall (nondisturbed flow). (c) Disturbed turbulent flow with separation, recirculation, and reattachment, showing complex velocity field. (Adapted from Heitz [18].)

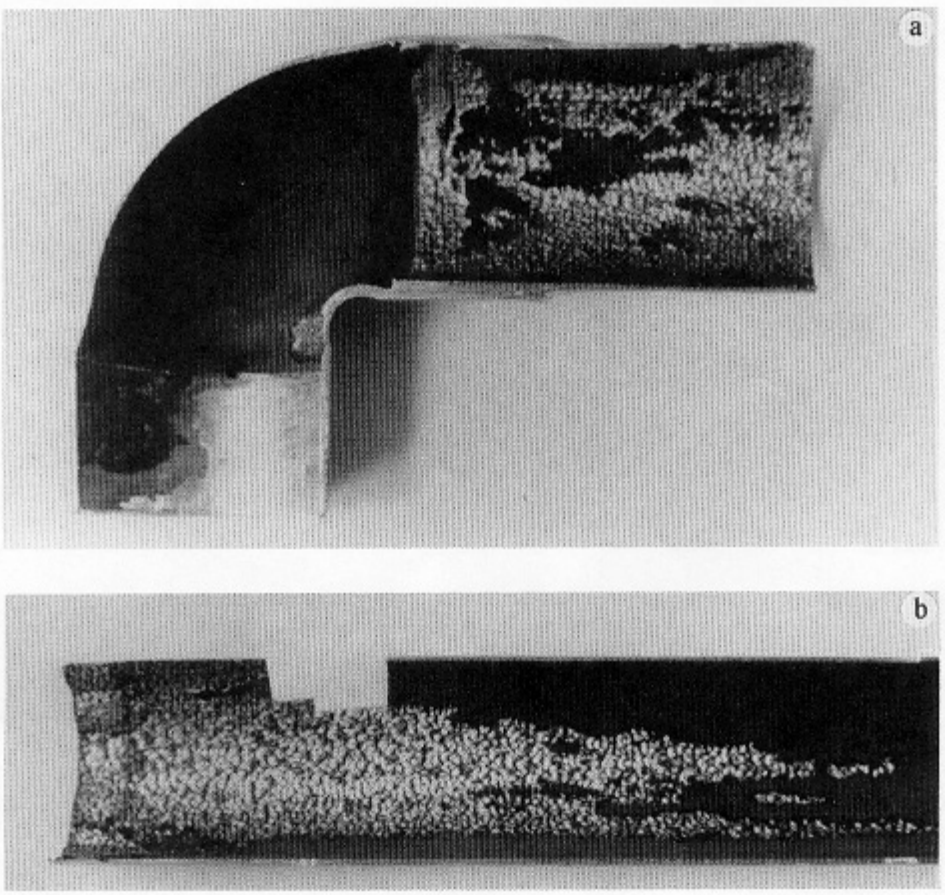

FIGURE 2. Erosion–corrosion of 53-mm copper tubing by potable water. (a) The attack started at the step where the tubing fitted into the elbow. (b) Once started, the attack progressed along the tube as a result of additional disturbed flow created by the erosion–corrosion roughened surface.

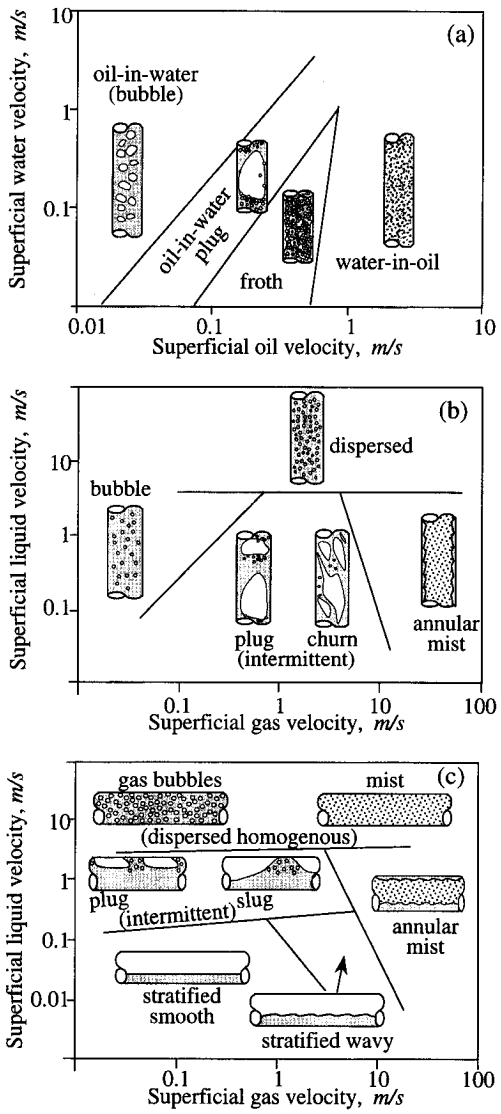

FIGURE 3. Qualitative two-phase flow structures in pipes. (a) Oil–water in vertical pipe, (b) liquid–gas in vertical pipe, (c) liquid–gas in horizontal pipe. (Adapted from Lotz [2], Weisman [3], and Govier and Aziz [4].)

C. PROTECTIVE FILMS

Most metals and alloys used in industry owe their corrosion resistance to the formation and retention of a protective film. Protective films fall into two categories:

1. The relatively thick porous *diffusion barriers*, formed on carbon steel (red rust) and copper (cuprous oxide).
2. The thin invisible *passive films* on stainless steels, nickel alloys, and other passive metals such as titanium.

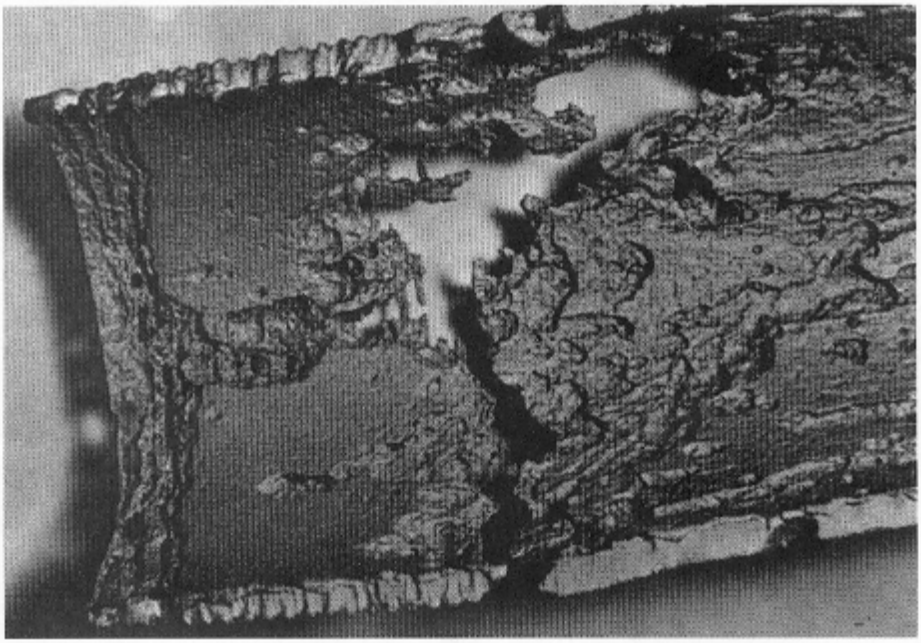

FIGURE 4. Erosion–corrosion of 115-mm API L-80 oil well tubing. Environment: Crude oil/CH_4/CO_2 and 1% H_2O in tight emulsion; temperature 200°C; velocity 6.4–7.9 m/s. Corrosion rate >10 mm/y. Remedy: Continuous inhibitor injection. (From Houghton and Westermark [6]. Reprinted, by permission of NACE International.)

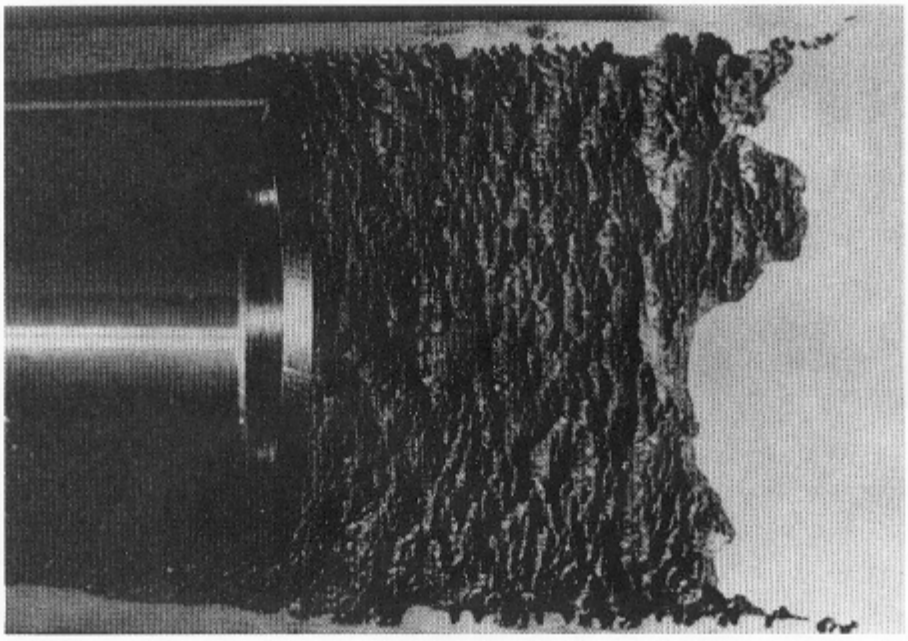

FIGURE 5. Impingement-type erosion–corrosion of AISI 4140 (UNS 941400) 115-mm flow coupling and subsurface safety valve in natural gas condensate production. Minor species: CO_2 and H_2O. Temperature: 79°C. Exit velocity from valve 91 m/s. Remedy: replacement with 13Cr martensitic ss. (From Houghton and Westermark [6]. Reprinted, by permission of NACE International.)

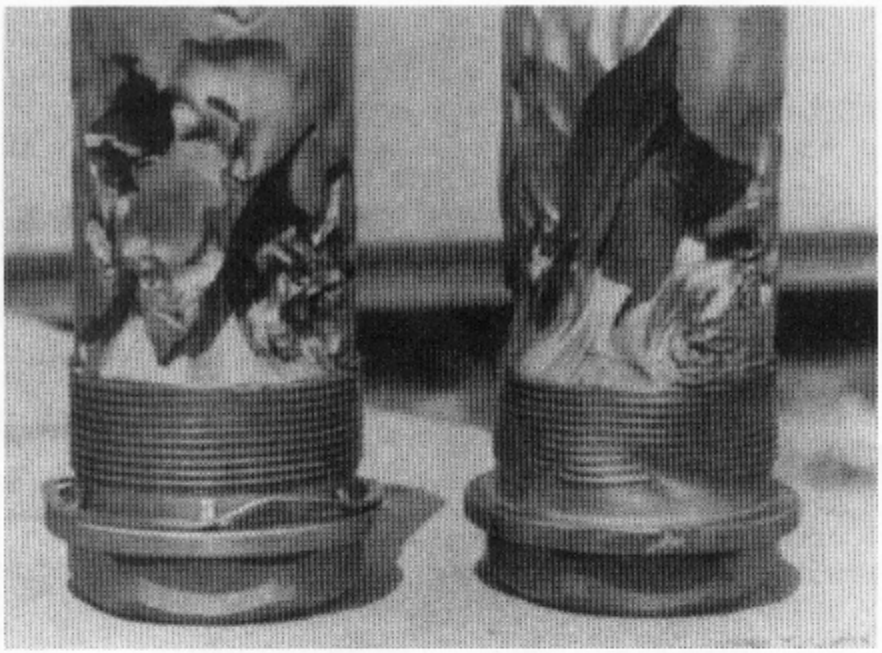

FIGURE 6. Erosion of tungsten carbide choke beans inside a steel holder from an oil well with sand production. Note the highly polished, streamlined appearance of the erosion pattern. Subcritical flow occurred in this well and these assemblies lasted between 6 and 9 months. (Smart [7]. Reprinted, by permission of NACE International.)

Diffusion barriers are formed by anodic dissolution followed by precipitation whereas passive films are formed by direct oxidation without the metal ions entering the solution. The softer thicker diffusion barriers are more easily damaged and more slowly repaired than the passive films, and passive alloys can withstand much more severe service conditions.

D. EROSION–CORROSION RATE

The effect of film destruction on the corrosion rate is illustrated by the following example. Carbon–steel pipe carrying water is usually protected by a film of rust, which slows down the rate of mass transfer of dissolved oxygen to the pipe wall. The resulting corrosion rates are typically < 1 mm/y (or < 40 mils/y). The removal of the film by a flowing sand slurry gives corrosion rates of the order of 10 mm/y (400 mils/y) in addition to any erosion of the underlying metal [12]. When corrosion is controlled by the rate of dissolved-oxygen mass transfer the corrosion rate can be calculated by the application of well established mass transfer correlations of dimensionless groups. In general,

$$\mathrm{Sh} = \alpha\, \mathrm{Re}^{\beta}\, \mathrm{Sc}^{\gamma}$$

where

$\mathrm{Re} = l u_t \rho/\mu$, Reynolds number, ratio of inertial forces to viscous forces

$\mathrm{Sc} = \mu/\rho D$, Schmidt number, ratio of momentum diffusivity to mass diffusivity

$\mathrm{Sh} = kl/D$, Sherwood number, ratio of convective mass transport to diffusive transport

k = mass transfer coefficient (m/s)

l = characteristic dimension (e.g., pipe diameter) (m)
D = diffusion coefficient (m^2/s)
u_b = bulk flow velocity (m/s)
μ = viscosity (Pa s)
ρ = density (kg/m^3)
α, β, γ = experimental constants

The Berger–Hau [13] correlation, one of the most widely accepted mass transfer correlations for fully developed turbulent flow in smooth pipes, gives $\alpha = 0.0165$, $\beta = 0.86$ and $\gamma = 0.33$. Based on the above correlation, a corrosion rate (CR in mm/y) calculated using the rate of mass transfer of dissolved oxygen to a film-free carbon–steel pipe wall, is given by

$$CR = 4923\, C_b (D_{O_2}/d) \mathrm{Re}^{0.86}\, \mathrm{Sc}^{0.33}$$

where

C_b = bulk oxygen concentration (mol/m^3)
D_{O_2} = diffusion coefficient for oxygen in water (m^2/s)
d = pipe diameter (m)

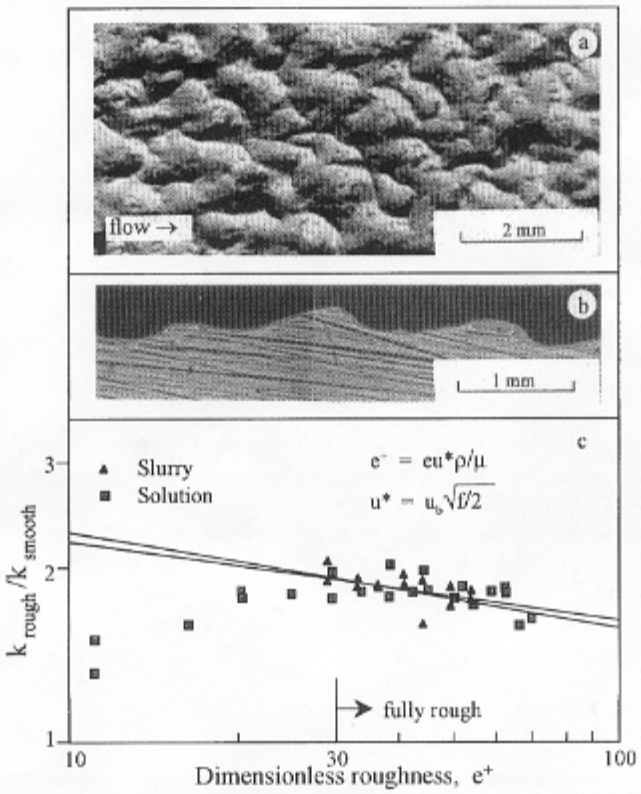

FIGURE 7. Effect of pipe-wall roughness on mass transfer rates. (a) Rough surface, preroughened by erosion–corrosion prior to mass transfer study. (b) Roughness profile details: roughness height, $e \approx 0.2$ mm, pitch/height in the range 5–10. (c) The ratio of measured mass transfer coefficients for preroughened and smooth surfaces at pipe wall. (Adapted from Postlethwaite and Lotz [17].)

This calculation assumes that two-thirds of the oxygen reaching the wall is used in oxidizing the iron to ferrous ions and that one-third is used in the oxidation of the ferrous ions to ferric ions close to the wall [12]. On this basis, a 100-mm diameter pipe carrying an aerated aqueous solution with $C_b = 8\,\text{ppm} \equiv 0.25\,\text{mol/m}^3$ of dissolved oxygen, $D_{O_2} = 2 \times 10^{-9}\,\text{m}^2/\text{s}$ flowing at 2 m/s would corrode at 7 mm/y.

The above calculation demonstrates the aggressive nature of erosion–corrosion and gives an indication of the high and unacceptable rates of corrosion whenever a protective film is damaged by erosion. Uniform erosion–corrosion and fully developed mass transfer are assumed. In practice, erosion–corrosion often occurs under disturbed flow conditions at localized areas. Consider, for example, iron, where the rust film formed at ambient temperatures is a poor cathode for oxygen reduction. The rate of oxygen mass transfer (and corrosion) at the small surface area where the protective film is removed will be substantially enhanced by

The disturbed flow effect [9, 14, 15].

The mass transfer entrance length effect [16].

The surface roughness effect [17] shown in Figure 7.

In addition, the situation may be complicated by the formation of flow-induced macroscopic corrosion cells following localized film disruption with differing behavior observed for copper and iron alloys [18].

E. RELATIVE ROLES OF EROSION AND CORROSION

The *accelerated corrosion*, following damage to the protective film, may be accompanied by *erosion* of the underlying metal. In some cases, the erosion of the base metal is not a factor. In other cases, erosion is the predominant factor and a wide spectrum of behaviors is observed [19]. The relative roles of corrosion and erosion following damage to the protective film can be estimated, Table 1, on the basis of the exponent y in the relationship between the metal loss rate and the bulk flow velocity, u_b [2]:

$$\text{erosion} + \text{corrosion} \propto u_b^y$$

The value of y will depend on the relative contributions of corrosion and erosion to the total metal loss.

In disturbed flow it is the flow characteristics in the direct vicinity of the wall rather than the bulk flow velocity that are important. In practice, however, the superficial flow velocity is the flow parameter that is readily measured and controlled [2].

TABLE 1. Flow Velocity as a Diagnostic Tool for Erosion–Corrosion Rates Following Damage to the Protective Film

Mechanism of Metal Loss	Velocity Exponent, y
Corrosion	
Liquid-phase mass transfer control	0.8–1
Charge-transfer (activation) control	0
Mixed (charge/mass transfer) control	0–1
Activation/repassivation (passive films)	1
Erosion	
Solid-particle impingement	2–3
Liquid droplet impingement in high-speed gas flow	5–8
Cavitation attack	5–8

F. EROSION–CORROSION MECHANISMS

The source of the various *mechanical* forces involved in the erosion of protective films and/or the underlying metal at flow-system walls (Fig. 8) are

Turbulent flow, fluctuating shear stresses, and pressure impacts.

Impact of suspended solid particles.

Impact of suspended liquid droplets in high-speed gas flow.

Impact of suspended gas bubbles in aqueous flow.

The violent collapse of vapor bubbles following cavitation.

Flow-enhanced film dissolution and thinning is a "chemical" form of protective film erosion leading to accelerated corrosion of the underlying metal.

1. Turbulent Flow

Erosion–corrosion occurs in single-phase turbulent pipe flow. The exact mechanism of protective film damage is in doubt. There is uncertainty regarding the roles of mechanical forces and mass transfer in film disruption [20–22] since both are directly related to the turbulence intensity.

Distinct "breakaway" velocities above which damage to normally protective films occurs in copper alloy tubes are observed [20] and this gave rise to the concept of a *critical shear stress* for film disruption.

The wall shear stress, τ_w, for flow in pipes is given by

$$\tau_w = f(\rho u_b^2/2)$$

where f is the Fanning friction factor [23]. In general [24],

$$f = f(\mathrm{Re}, \varepsilon/d, \varepsilon'/d, m)$$

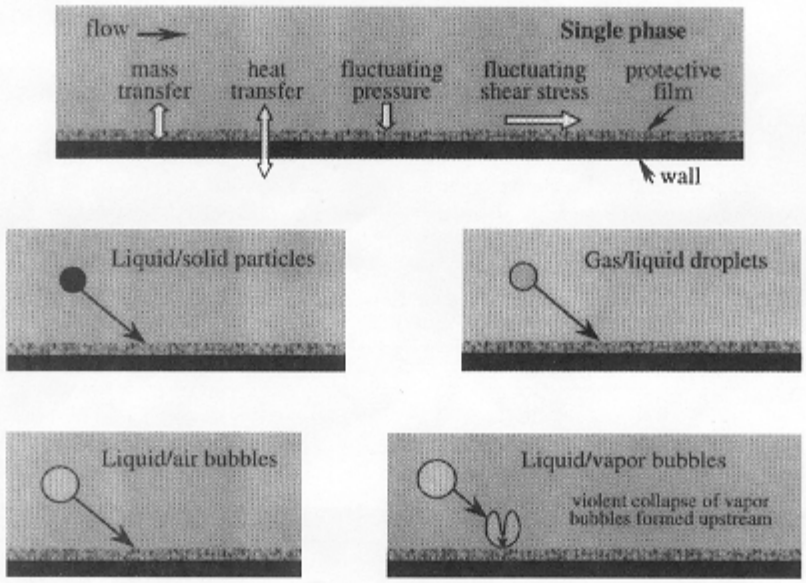

FIGURE 8. Interaction of flowing fluid with wall of the flow system leading to erosion–corrosion. (Adapted from Heitz [18].)

where ε is a measure of the size of the roughness projections, ε' is a measure of the arrangement of the roughness elements, and m is a form factor that is dependent on the shape of roughness elements.

For flow in smooth pipes,

$$f = 0.046\,\mathrm{Re}^{-0.2}$$

is valid to higher Reynolds numbers than the Blasius equation [25]. Values of the Fanning friction factor for both smooth and rough commercial pipes and tubes can be obtained from a Moody* chart [23]. For fully rough† pipe flow f is independent of Re, and $\tau_w \propto u_b^2$.

Early attempts [26] to correlate film damage with the wall shear stresses in pipe flow based on the bulk flow velocity resulted in shear stress values, Table 2, that seem too low [20] to strip a corrosion product film unless it is very loosely adhering. The "breakaway" velocities, u_{cr}, shown in Table 2, were calculated from critical shear stress values. Design velocities for heat-exchanger tubing should not be based on critical shear stress values for fully developed *nondisturbed* tube flow since the flow is both developing and disturbed at the tube inlets. In fact, disturbed flow must be allowed for in most industrial systems. The values calculated from $0.5\,u_{cr}$ are also shown and can be compared to the "maximum recommended design velocities" [27]. The design velocity must clearly be chosen with care, with previous experience in similar systems being the best guide.

In reality, there are fluctuating shear stresses and pressures at the wall. The largest values are obtained during quasicyclic bursting events close to the wall, which are said to be responsible for most of the turbulent energy production in the entire wall-bounded shear flow [28, 29]. This is true of both nondisturbed and disturbed pipe flows. In practice, film removal in single-phase aqueous flow is invariably associated with the vortices created under disturbed flow conditions produced by sudden macro or microscale changes in the flow geometry. It is quite difficult to avoid microscale geometrical imperfections in a flow system during experimental studies to determine critical shear stress values.

The films on passive alloys, such as stainless steels, are not usually damaged by single-phase aqueous flow [18, 30]. Rust films on carbon steel at ambient temperature are more mechanically

TABLE 2. Critical Flow Parameters for Copper Alloy Tubing in Seawater

Alloy	Critical Shear Stress[a] (N/m^2)	Critical Velocity 25-mm tube[b] (m/s)	"Design" Velocity[c] Based on 50% $\tau_{w,crit}$ (m/s)	Accepted Maximum Design Velocity[d] (m/s)
Cupro nickel with Cr	297	12.6	8.6	9
70–30 Cupro nickel	48	4.6	3.1	4.5–4.6
90–10 Cupro nickel	43	4.3	2.9	3–3.6
Aluminum bronzes				2.7
Arsenical Al brass	19	2.7	1.9	2.4
Inhib. Admiralty				1.2–1.8
Low Si bronze				0.9
P deoxidized copper	9.6	1.9	1.3	0.6–0.9

[a] From Efird [26], rectangular duct.
[b] Critical velocities, calculated using Efird shear stress values.
[c] Calculated values based on 50% of critical shear stress.
[d] "Accepted" maximum tubular design velocities [27].

* The Fanning friction factor should not be confused with the Darcy friction factor that is four times greater and is used on some Moody charts.

† In flow through rough pipes, the roughness elements penetrate the boundary layer into the main fluid stream at high Re resulting in form drag and under fully rough conditions the viscous forces become negligible.

stable than the protective film formed on copper. The compactness and protectiveness of rust films (FeOOH) increase with velocity [31]. The magnetite films formed in high-temperature water and sulfide films formed on carbon steel have a high mechanical stability in single-phase aqueous flow [18]. Thus the velocity limit, around 1 m/s, suggested for copper tubing [32, 33] is lower than the velocities tolerated by carbon–steel and low alloy piping at ambient temperatures and much lower than the allowable velocities at elevated temperatures.

In *slug flow* in horizontal gas/liquid pipelines [Fig. 3(c)], large shear stress values (with a major dynamic component) will be observed at the top of the pipe [2]. The slugs of liquid travel at much higher velocities than is encountered in normal liquid flows, and have been associated with severe erosion–corrosion problems in oil/gas production systems.

2. Solid Particle Impingement

The impingement of solid particles, entrained in a flowing liquid, can damage both types of protective films (thick diffusion barriers and thin passive films) leading to erosion–corrosion. The particles may also erode the metal adding to the overall metal loss.

As might be expected, the erosion rate, ER, is a function of the kinetic energy of the impinging particles (proportional to u_p^2) and the frequency of impacts (proportional to u_p), and to a first approximation [2]:

$$\mathrm{ER} \propto u_p^3$$

The kinetic energy of the particle, normal to the wall, will be determined by the *impact velocity* and *impact angle* along with the particle *density* and *size*. Erosion of brittle materials by slurries increases with the particle impact angle to reach a maximum at 90°. Ductile materials develop erosion maxima in the range 15–40° [18]. The impacts of small particles in aqueous slurries may be damped by the presence of the boundary layer at the system wall [18, 34]. In practice, hard abrasive slurries are often transported through mild-steel pipes with the particles finely ground. The erosion is reduced because of the smaller particle size and the lower flow velocity required to maintain the solids in suspension [35].

Both the impact velocity and the impact angle will be strongly affected by disturbed flow and this is where the most severe erosion is found in practice. Impact angles in nondisturbed turbulent pipe flow are $< 5°$ whereas a wide range of angles will be encountered in disturbed flow [36]. Thus carbon–steel pipe can transport sand slurries with an *erosion* rate of < 1 mm/y under nondisturbed flow conditions [12, 34] (Fig. 9). Similar sand-slurry flows caused the erosive failure of a reducer located immediately downstream of a T junction and pinch valve in eight days illustrating [Fig. 9(c)] the very severe erosion that can occur under disturbed flow conditions [34].

In dilute slurries < 5 vol% solids, the impact frequency and erosion rate are proportional to the *solids concentration* [8]. At higher concentrations particle-particle interference reduces this dependency [35, 37].

The *shape* of the particle and the *microroughness* of the particle surface [38] influence the effective forces generated at the wall by the impact. Thus rounded sand particles, which were superficially smooth, resulted in erosion rates [37] two orders of magnitude greater than the erosion by glass beads in the same system. The difference in behavior was related to the microroughness of the sand particles, which could be seen at high magnification under an electron microscope.

The damage done will be strongly related to the *relative hardness* (Fig. 10) of the impinging particles and the flow system walls. Erosion drops dramatically [35], when the impacting particles are softer than the wall. For example, the Mohs hardness of coal is ~ 2, iron ore 6 and sand 7. Carbon–steel pipe API 5LX or similar used for long-distance slurry transportation [39] has a Brinell hardness ~ 120 (Mohs hardness ~ 3). Thus it might be expected that whereas coal slurries could possibly damage rust films and cause accelerated corrosion, there would be no erosion of the underlying metal. Sand, iron ore, and other hard minerals could cause both accelerated corrosion and

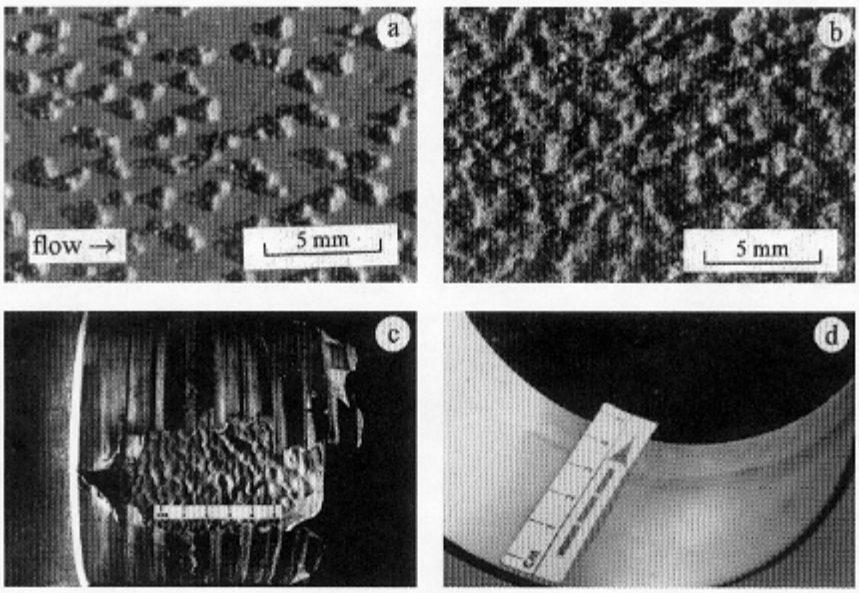

FIGURE 9. Variations in erosion–corrosion wear patterns in a 100-mm diameter pipe carrying an abrasive sand slurry. (a) Developing erosion–corrosion wear pattern in nondisturbed flow showing individual pits. (b) Fully developed erosion–corrosion wear pattern with roughened surface. (c) Effect of disturbed flow, with failure of reducer placed downstream of T junction and pinch valve in 8 days. (d) Erosion pattern with the corrosion component suppressed by application of cathodic protection. *Note*: Cathodic protection not suitable for the inside of pipelines. (From Postlethwaite et al. [34]. Reprinted, by permission of NACE International.)

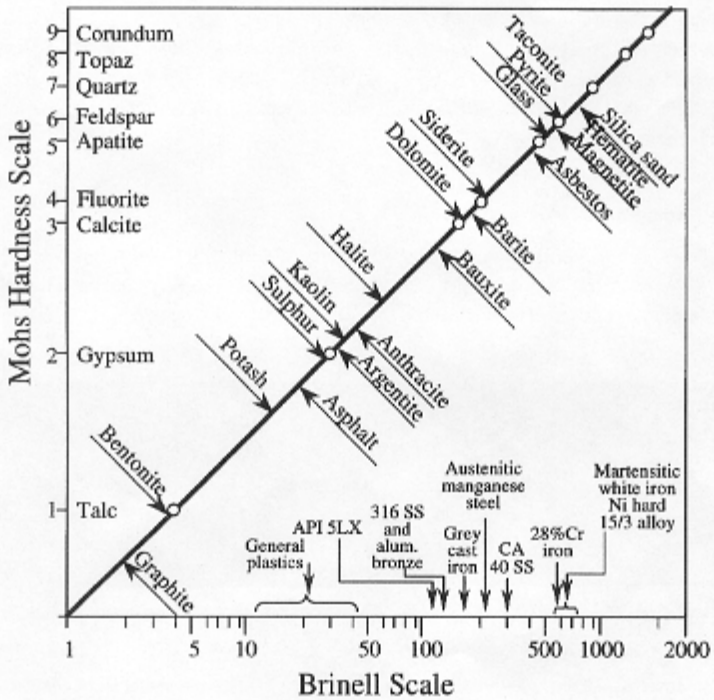

FIGURE 10. Approximate comparison of hardness values of various common minerals and metals. (Adapted from Wilson [69].)

erosion. A complicating factor sometimes found with coal and other slurries is the presence of small amounts of silica and other hard minerals.

The ability of impacting particles to damage or interfere with the development of protective films is difficult to quantify in the absence of information regarding the mechanical properties of the in situ films [18], and in the case of passive films the damage and healing characteristics. In general, impacting particles will often damage protective films even under circumstances where they cannot erode the base metal. Lotz [2] proposed that solid-particle damage to passive films, with subsequent rapid repassivation will result in a corrosion rate directly proportional to the particle concentration and flow velocity. Any erosion of the underlying metal will increase the exponent on the velocity. Metal loss measurements [40] with dilute slurries in nondisturbed turbulent pipe flow resulted in values of the velocity exponent up to 3 for corrosion resistant materials and values down to 1.4 for less corrosion resistant materials. Measurements [12] with sand slurries in carbon–steel pipes gave an exponent close to 1 with erosion playing a minor role at the velocities involved. These two sets of results indicate the utility of using the velocity as a diagnostic tool to determine the relative roles of accelerated corrosion and erosion of the underlying metal discussed above.

Sand particles can play a major role in the erosion–corrosion of oil/gas production systems [5]. At low velocities accelerated corrosion is the major factor, whereas at the high velocities found in chokes, erosion can lead to the rapid destruction of the component [7] as shown above in Figure 6.

3. Liquid Droplet Impingement

Erosion by impinging liquid droplets carried in high-speed vapor or gas flows is usually called liquid impingement attack. The attack involves the exposure of the solid to repeated discrete impacts by liquid droplets, which generate impulsive and destructive contact pressures, far higher than those produced by steady flows [41]. Impingement erosion has been a problem with low-pressure steam turbine blades operating with wet steam and rain erosion of aircraft and helicopter rotors. Liquid droplet impingement attack has much in common with cavitation attack [42] in terms of both the mechanism, which is largely one of deformation erosion, and the morphology of the attack, with continued deepening of discrete sharp edged pits, which coalesce to a honeycomb-like appearance [43] (Fig. 11). Corrosion, as with cavitation attack, usually plays a secondary role, which varies with the hydrodynamic intensity.

4. Air Bubble Impingement

The erosion–corrosion of copper alloy heat-exchanger-tube inlets has been linked [10] to the local damage of protective films by impinging air bubbles, which have a substantial radial velocity component immediately downstream from the tube-sheet inlets. Nitrogen bubbles [20] have a similar

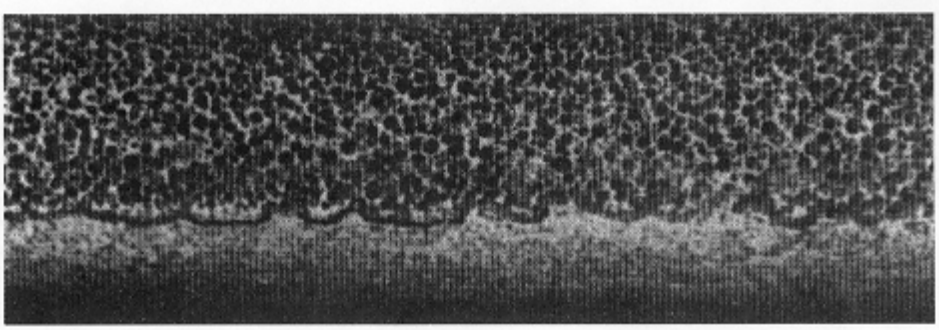

FIGURE 11. Impingement attack of outside of cupro-nickel tube by wet steam. (From Century Brass [43].)

effect and it seems clear that the damage to the film is hydro-mechanical. The attack, which initially takes the form of isolated "horseshoes", spreads to a general roughening characteristic of erosion–corrosion. Similar horseshoe patterns were produced by microturbulence at grain boundaries on dissolving solid benzoic acid [10] illustrating the role of microturbulence and hydrodynamics in the erosion–corrosion pattern produced on copper tubing.

5. Cavitation

Cavitation attack takes the form of steep sided pits, as shown in Figure 12 [33], which sometimes coalesce to form a honeycomb-like structure [42]. The attack is the result of the violent collapse of *vapor cavities*, or bubbles, < 1 mm diameter [44, 45], that are formed in a flowing liquid when the hydrostatic pressure drops below the vapor pressure of the fluid. The cavities are carried downstream to higher pressure regions where collapse occurs. The *dynamic forces* associated with the collapse of the cavities at the walls of the system, lead to high frequency fatigue–stress damage. The shock waves from spherical collapse and microjets from asymmetrical collapse have both been suggested as the cause of the damage. The inconsistencies with previous theories are now considered to be explained by the concept of the collapse of clusters of cavities in concert [44]. Cavitation attack often involves an induction period, especially for ductile materials, following which the erosion rate is nonlinear [46]. The time dependency is similar to that observed in the related phenomenon of liquid droplet impingement [41].

The cavitation resistance of metals and alloys spans a range of at least two orders of magnitude [41, 45], far greater than the conventional strength properties. The velocity exponent varies widely with values usually given in the range 5–8 [45]. With such a high-velocity exponent, a small change

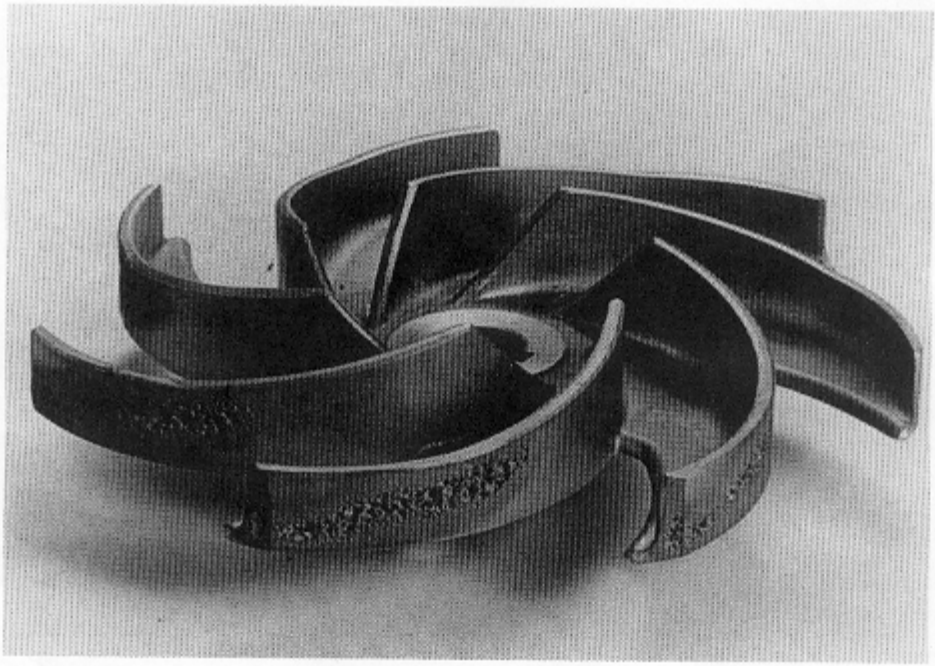

FIGURE 12. Cavitation attack of a stainless steel (AISI 316) pump impeller. Environment: skimmed milk @ 70°C. Remedy: Replace impeller by one made of Teflon PFA (perfluoroalkoxy). (From [33] reprinted from E.D.D. During, Corrosion Atlas: A Collection of Illustrated Case Histories, Vol. 2: Stainless Steels and Non-ferrous Materials, Copyright © 1988, with permission from Elsevier Science.)

in operating conditions could lead to serious problems. The effects of velocity should not be considered independently of pressure, since the cavitation number, σ, which is a measure of the intensity of cavitation, is a function of both parameters [46]:

$$\sigma = (p - p_v)/0.5\,\rho u^2$$

where p and p_v are the absolute static pressure and the liquid vapor pressure, respectively, and u the free stream velocity. When $\sigma = 0$, the pressure is reduced to the vapor pressure and cavitation will occur.

The role of corrosion, which varies with the hydrodynamic intensity, is difficult to predict [46]. Under some circumstances it is claimed that hydrogen bubbles liberated by the application of cathodic protection provide a mechanical cushion reducing the cavitation damage [42] in addition to the normal cathodic protection effect. In other cases, corrosion may contribute to the overall attack directly, following damage to protective films. In the latter case, the velocity exponent for a given system might be expected to be reduced as the corrosion component increases as is the case with erosion–corrosion by solid particles discussed above.

Cavitation is a problem with ship propellers, hydraulic pumps and turbines, valves, orifice plates and all places where the static pressure varies very abruptly on the basis of the Bernoulli* principle:

$$gz + u^2/2 + p/\rho = \text{const}$$

where z is the elevation. Strictly speaking, the Bernoulli equation applies to flow along a streamline,† however, in turbulent flow the bulk flow velocity u_b can be used with little error. Thus the increase in the velocity as the liquid is accelerated through an orifice plate or over the curved impeller of a centrifugal pump results in a fall in the static pressure. As the liquid slows down, after it passes the vena contracta or approaches the volute in the pump, the pressure rises again leading to the collapse of the cavities described above. Friction losses and the resulting drop in pressure in pump suction lines can lead to serious cavitation damage at the pump inlet. Objectionable noise, vibration, and loss of equipment performance often accompany cavitation attack. Cavitation attack also occurs at vibrating solid surfaces such as the cooling-water side of diesel engine cylinder liners [46] and on the shell side of heat-exchanger tubing [47].

6. Wire Drawing

Wire drawing is a form of erosion–corrosion found in very high velocity fluid flow through small gaps. This type of attack, which is difficult to classify, takes the form of single or multiple clean smooth grooves, as shown in Figure 13 [48]. The attack could involve liquid droplet impingement attack when it occurs at valve seats with escaping steam and cavitation attack when it occurs with a single-phase fluid system [41]. The fluid may be aqueous or nonaqueous.

7. Flow-Enhanced Film Dissolution

Flow-enhanced film dissolution (with thinning) is a "chemical" form of protective film erosion leading to accelerated corrosion. This type of erosion–corrosion has caused some serious problems in carbon–steel lines (protected by magnetite films) carrying hot (100–250°C) deoxygenated water

* The engineering form of the Bernoulli equation includes terms for shaft work and friction losses (Perry and Green [23]).

† The use of the term streamline in turbulent flow is confusing to some that might think the term applies only to laminar (viscous) flow. A streamline is a continuous line drawn through a fluid so that it has the direction of the velocity vector at every point. There can be no flow across a streamline. When very small solid particles are used to study the flow pattern, by the use of laser Doppler anemometry, the particles follow the streamlines [24].

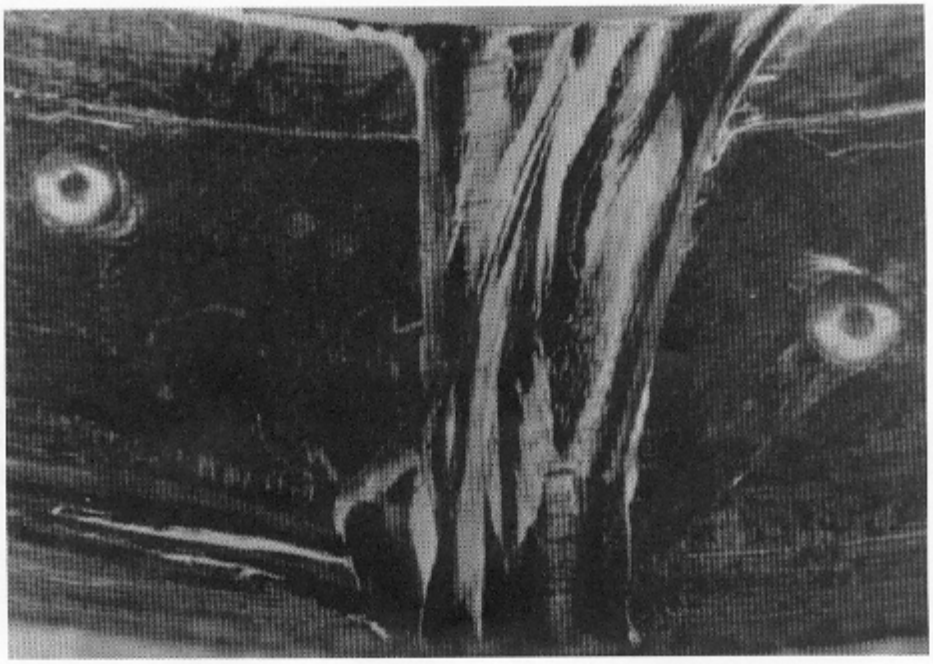

FIGURE 13. Wire drawing in a bronze cam ring for a hydraulic pump. (From Glaeser [48]. Reprinted, by permission of NACE International.)

or wet steam in fossil fueled and nuclear power plants.* The problem occurs at locations with high mass transfer rates, corresponding to highly turbulent flow conditions found at bends, and downstream of pumps, valves, and orifice plates. At these locations the film is dissolved more rapidly, and a higher anodic current is needed to replenish the protective film. The resulting steady state involves a thinner and less protective film and a much higher corrosion rate leading to rapid localized thinning of the equipment walls.

At high velocities in wet steam, convective dissolution of magnetite films is said to be supplemented by oxide fatigue by liquid droplet impacts. At the outside of bends, liquid droplets under the influence of secondary flow and centrifugal acceleration impinge on the magnetite, fatiguing it and causing it to erode away, exposing new metal to the steam. On the inside of the bend, where an inward flowing stagnation point occurs with a very high mass transfer coefficient, convective dissolution is the major mode of oxide damage [49]. Giralt and Trass [50] suggested that the contribution of dissolution can be additive to film erosion and sometimes acts in a synergistic way by loosening the crystal grains of the film, making them more prone to erosion.

The effect of velocity on flow-enhanced film dissolution is complex and, although much has been learned with respect to the identification and control of this problem, much more work is required on the fundamentals of the processes involved [51].

G. EROSION–CORROSION RECOGNITION AND CONTROL

A major prerequisite for the control of erosion–corrosion is the recognition or determination of the relative roles of accelerated corrosion and erosion. Only then can the appropriate action be taken.

* The term flow-accelerated corrosion (FAC) has been used to describe this specific problem (EPRI [51].) However the term erosion-corrosion is normally used in the literature and is the preferred term. The term FAC could relate to a whole range of flow-dependent corrosion processes in addition to its application to flow-enhanced film thinning.

If accelerated corrosion following damage to protective films is the problem there are two alternatives:

1. Take steps to avoid damage to the film.
2. Accept the film damage and use corrosion control methods.

If erosion of the underlying metal is a major factor, design and materials selection solutions should be sought.

Recognition of the type of erosion–corrosion is sometimes relatively straightforward. Erosion–corrosion by both single-phase aqueous flow and suspended solids is characterized by the presence of smooth grooves, gullies, shallow teardrop shaped pits, and horseshoe shaped depressions most often with an obvious flow orientation. The characteristic pattern of attack often starts at isolated spots on the metal surface and subsequently spreads to a general roughening of the surface [10, 34]. With cavitation and liquid droplet impingement attack, the damage starts in the form of steep sided pits, which may coalesce into a honeycomb-like structure. "The Corrosion Atlas" [33] and the NACE International, "Corrosion Recognition and Control Handbooks" [47, 52] contain photographs of all the various forms of erosion–corrosion with suggested control methods built around a large number of case histories.

1. Control of Turbulent Flow Attack

In single-phase aqueous flow, the erosion–corrosion of metals such as copper tubing, is a process of accelerated corrosion following erosion of the protective film. Control of this type of attack is usually achieved by modifying the design of the system to reduce the hydrodynamic forces and/or by choosing an alloy with a more erosion-resistant film.

1.1. Design Design factors, for example, for copper tubing carrying potable water are the control of the velocity and the minimization of abrupt changes in the flow system geometry. Maximum velocities in the range 0.8–1.5 m/s have been suggested [32, 33]. The tubing should be reamed where it is pushed into fittings such as elbows prior to soldering [53] to mitigate the erosion–corrosion shown in Figure 2. Recent studies [22] have shown that 1 mm forward or backward facing steps are sufficient to initiate film disruption. Reaming in excess of that required to remove the burring on cut tubing may be required to prevent erosion–corrosion. Plastic inserts can be used to solve heat-exchanger-tube-inlet problems.

1.2. Materials Materials selection could involve, for example, the substitution of copper tubing in hot water distribution systems by stainless steels or plastics [33]. As noted above, only in extremely severe conditions would single-phase aqueous flow damage the passive film on stainless steels leading to erosion–corrosion. The possible pitting and crevice corrosion of stainless steels in the presence of chlorides should be taken into consideration. A range of copper alloys with increasing velocity limits can be used in heat exchangers, Table 2. If a very high velocity is required, in a corrosive environment, stainless steel, nickel alloy or titanium tubes can be considered [54, 30].

1.3. Inhibitors Inhibitors are used in recirculating cooling water systems and steam condensate return lines but find limited application in once-through production systems because of the cost. A notable exception is the extensive use of inhibitors in oil/gas production.

1.4. Cathodic Protection Cathodic protection has very limited throwing power down the inside of pipes and other restricted geometries. Impressed systems can be used in heat-exchanger water boxes to protect the important entrance length region for copper alloy tubes [10, 55] carrying seawater. Care must be taken to avoid hydrogen evolution, which can lead to the formation of air/

hydrogen pockets at dead zones [10]. In addition to safety problems, hydrogen can lead to the embrittlement of titanium and other alloy tubing.

2. Control of Solid Particle Impingement Attack

Erosion–corrosion problems observed in the presence of solid particles suspended in aqueous solutions are more difficult to solve. The relative role of corrosion and erosion can often only be assessed following testing involving weight loss measurements to determine the total loss with simultaneous electrochemical measurements (polarization resistance) to determine the contribution of corrosion [12, 56]. The relative importance of erosion and corrosion will vary between nondisturbed and disturbed flow and testing should be done in a flow system that simulates both the chemical and the hydrodynamic conditions found in the full-scale-process equipment.

2.1. Corrosion Control Corrosion can be controlled by the use of inhibitors and/or solution conditioning. Some inhibitors work very well in the presence of very abrasive slurries including silica, which is one of the most common abrasive components. Chromates and nitrites at high concentrations act as passivating inhibitors [57], whereas chromates at low concentration act as cathodic inhibitors [58, 59], and were used in the first long distance coal-slurry pipeline [60]. Chromates are of course toxic and very low effluent limits < 0.05 ppm have been set in some jurisdictions [61]. Non-chromate inhibitors used in cooling water systems, zinc, sodium tripolyphosphate ($Na_5P_3O_{10}$), and nitrilotris (methylene) triphosphonic acid (NTMP), $N[CH_2PO(OH_2)]_3$, showed little benefit [58] in sand or coal slurries when used alone or along with chromates in contrast to the synergistic effect normally observed in cooling water.

Solution conditioning involves raising the pH and/or deaeration. Both of these methods of corrosion control have been applied to long-distance slurry pipelines. A problem with raising the pH, to control corrosion, is the greater likelihood of pitting at elevated pH values where thick scales are more easily formed. Indeed, pitting caused some concern with the Bougainville copper concentrate line [62] which was treated with lime to maintain the slurry at $pH > 9.5$. Temporary overdosing with lime led to calcium carbonate deposits in the first portion of the Samarco iron ore concentrate line [63], which was maintained at $pH \geq 10$. Deaeration can be achieved with oxygen scavengers, sodium bisulphite, or hydrazine or by nonchemical steam stripping or vacuum deaeration. The latter two methods of deaeration have not been used with slurry pipelines. They are used extensively for example with oil-well water-injection systems [64].

If the corrosion following the removal of the protective film is liquid-phase mass transport controlled, the flow velocity can be reduced. However, the effect of reducing the velocity will be of secondary importance to controlling the corrosion by inhibitors or solution conditioning. A lower limit is the velocity required to keep the particles in suspension [35]. For example [65] the flow of a 20 vol% silica-sand slurry, mean particle diameter 0.43 mm, in a 50-mm horizontal diameter pipe requires a minimum velocity of ~ 2 m/s and a 20 vol% slurry of iron ore concentrate, mean particle diameter, 0.04 mm, a minimum velocity of ~ 1.3 m/s. Lower velocities may result in the *sliding abrasion* of a horizontal pipe bottom. At velocities above the critical velocity to keep the particles in suspension, there is a large concentration gradient from the top to bottom of horizontal pipelines carrying commercial heterogeneous slurries [35]. This can result in a much different erosion–corrosion wear pattern and rate around the circumference of the pipe (Fig. 14).

If necessary more corrosion resistant materials than carbon–steel pipe can be chosen including, stainless alloys, ceramics (e.g., cast basalt lined pipe, Mohs hardness ~ 8) and plastics (e.g., high-density polyethylene pipe or polyurethane linings).

Stainless alloys, with their rapidly healing films, have a greater resistance to corrosion in slurries but the extra resistance comes at a cost that may not be acceptable. Ceramics and plastics may not have the mechanical and thermal properties for the construction of the particular process equipment. Long distance pipelines are constructed from carbon steel. More expensive alloys and lined pipe are

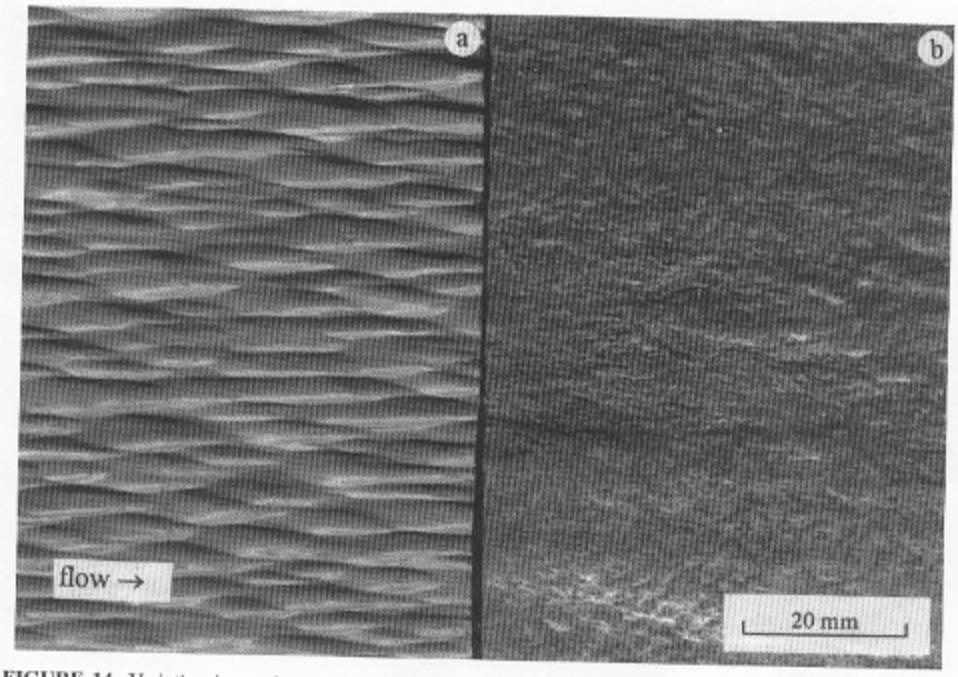

FIGURE 14. Variation in erosion–corrosion wear pattern around the circumference of a horizontal 200-mm diameter commercial pipeline carrying an abrasive mineral slurry. (a) Pipe bottom. (b) Pipe top. *Note*: The erosion–corrosion wear pattern in (a) is not characteristic of sliding bed wear. Sliding wear is characterized by long horizontal grooves.

an option for in-plant operations including tailings disposal. Titanium alloys perform well in flowing seawater with abrasive solids in suspension [66].

*2.2. **Erosion Control*** Erosion can be controlled by design and materials selection. Design involves optimizing the particle size (by grinding, where there is a choice of size) and the flow velocity [35]. The flow system geometry should be designed to minimize any effects of disturbed flow, for example, by using long radius elbows, gradual changes in the flow cross-section, and specifying maximum weld root protrusion. Other design possibilities are

Increasing the thickness of materials in critical areas.

Use of impingement plates to shield critical areas.

Acceptance of a high erosion rate with regular inspection and replacement may be less costly than using more expensive materials, and is a practice used extensively in the minerals processing and oil/gas industries.

In some situations pipe rotation for example to extend the life of tailings lines.

Since there is a major decrease in the erosion rate when the metal surface is harder than the particles it might be thought to be a simple matter to choose an alloy with a hard surface and eliminate the erosion problem. This is not the case for two reasons:

The hard alloys that resist erosion are generally cast alloys that are difficult to weld, often brittle and in general difficult to handle.

If corrosion is a factor the alloy must have a suitable corrosion resistance and many alloys that are hardened by the precipitation of carbides during solidification, have a relatively poor corrosion resistance.

Alloyed white cast irons (the most abrasion resistant iron-base alloys), including high-chromium, chrome-moly, nickel-chrome, and pearlitic white irons [67] are noted for their erosion resistance. The relationship between the Cr and C content of the high-chromium cast irons is complex. A high C content is required for the formation of carbides to give erosion resistance but this leaves less Cr in the matrix for corrosion resistance [68]. The minimum Cr content in the matrix to form a passive film is 12% and the Cr required to form carbides is $10 \times \%C$. The suggested minimum Cr for corrosion resistance is

$$\%Cr = (\%C \times 10) + 12$$

The erosion resistance increases and the corrosion resistance decreases with an increase in the C content and the alloy must be chosen carefully to accommodate the corrosive and erosive properties of the particular slurry being handled. Alloys containing 20–28% Cr and 2–2.5% C with 2% Mo have good resistance to slurry erosion–corrosion at pH values down to 4. Alloys with less C are required for more corrosive environments [68]. Ni-Hard alloys (4% Ni-2% Cr) find extensive use in abrasive service in sand and gravel pumps handling abrasive but mildly corrosive slurries [69]. Natural rubber is an alternative for pumps to handle abrasive slurries with particles < 3-mm diameter.

Both Stellite (a cast cobalt alloy) and silicon carbide have excellent erosion resistance in aqueous slurries along with excellent corrosion resistance and can be considered for use under severe service conditions in valves and pumps [33, 40].

3. Control of Liquid Droplet Impingement Attack

Impingement attack by liquid droplets suspended in high-speed gas flow can be controlled by *design* or *materials selection*.

Design involves optimizing the flow system geometry and the fluid dynamics [41] to reduce: the amount of impacting liquid; the angle of impact; and the droplet size. For example, design modifications in steam turbines operating with wet vapor in the low-pressure section have included: extracting moisture between blade rows; increasing axial spacing between stator and rotor; and local flame hardening or brazed-on shield of Stellite at the leading edge of the blade. Raising the temperature of the inlet gas above the dew point was suggested [47] as a remedy for the impingement attack of a process gas compressor. Impingement plates acting as flow deflectors can also be considered.

The behavior and range of materials utilized to solve high-speed liquid droplet impingement problems are similar to those chosen for resistance to cavitation attack. The "normalized erosion resistance" data shown in Figure 15 give an approximate ranking of materials to liquid droplet impingement and cavitation attack. Such data should be used with great care. Materials selection for turbines includes; the use of Stellite mentioned above; 12% chromium martensitic stainless steel, 17 Cr–4 Ni precipitation hardened stainless steel; and "self-shielding" blade alloys that harden under the action of impacts [41].

Liquid droplet impingement attack observed in annular mist flow [Fig. 3(b)] in oil/gas production systems is an erosion–corrosion phenomenon, which can be controlled by the use of inhibitors or the use of stainless alloys [7]. Not surprisingly this erosion–corrosion is found to be the most severe under disturbed flow conditions at threaded connections in down-hole tubulars and at elbows, valves and "Christmas trees" in above ground facilities.

4. Control of Cavitation Attack

Cavitation attack is usually controlled by design and materials selection. Tullis [70] has given an extensive discussion of the detailed design of pumps, valves, orifices, and elbows to avoid cavitation

problems. Air injection is sometimes used to control cavitation damage. Air injected into the separated flow regime cushions the collapse of the cavities. Cathodic protection has been used, with the protection attributed to cushioning by the hydrogen bubbles evolved in addition to the normal corrosion protection. While this might be satisfactory for a propeller in an open system the evolution of hydrogen in a closed system could be hazardous as well as leading to hydrogen blistering and embrittlement.

The range of materials available for solving cavitation–erosion problems is similar to those used for liquid droplet impingement as shown in Figure 15. There is a wide range of polymers with good resistance to cavitation–erosion in addition to excellent resistance to corrosion. For example, high-density polyethylene has a cavitation–erosion resistance similar to that of nickel-based and titanium alloys [45].

The major design parameter for centrifugal pumps to avoid cavitation damage is the available net positive suction head, ($NPSH_A$), the difference between the total pressure (absolute) and vapor pressure at the pump suction, expressed in terms of equivalent height of fluid, or "head" by

$$NPSH_A = (p/\rho g) + (u^2/2g) - (p_v/\rho g)$$

where

p = static pressure (absolute)
p_v = vapor pressure of the flowing fluid
ρ = density
g = gravitational acceleration
u = flow velocity

The $NPSH_A$ must exceed the value required by the pump, $NPSH_R$. The latter value varies with the flow rate and is a function of the pressure changes as the liquid accelerates over the curved impeller

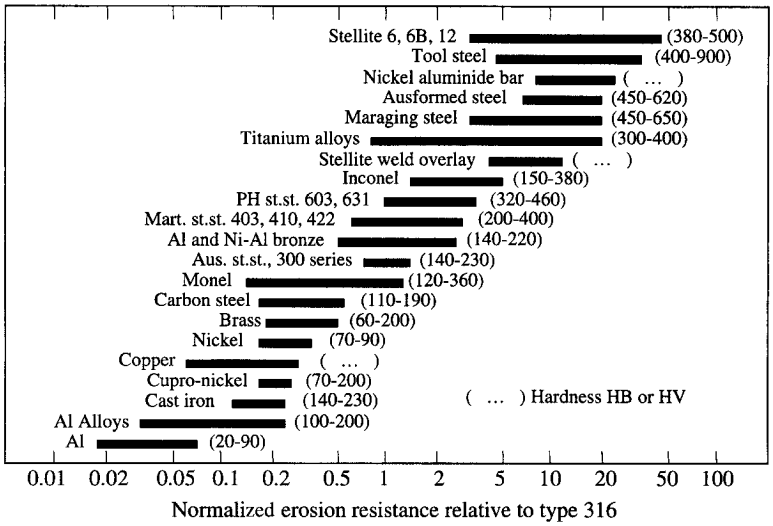

FIGURE 15. Normalized erosion resistance of various metals and alloys (the erosion resistance number according to ASTM G73). Selection of the data deduced by Heymann [41] from many sources, including both impingement and cavitation tests. Erosion test data are not very consistent, and the information herein should be used only as a rough guide. (Adapted from Heymann [41].)

and then decelerates as it approaches the volute. The $NPSH_R$ values, which are supplied by the pump manufacturers, are based on pump efficiency and not on the dangers of cavitation attack. Significant noise and cavitation may occur before the efficiency of the pump begins to decrease. Thus a substantial margin of safety is required if erosion–corrosion is to be avoided. In practice, some cavitation can usually be tolerated and pumps are operated in the NPSH range between cavitation inception and a point where damage is unacceptable [45, 70]. If it is wished to maximize efficiency of the pump operation, more cavitation can be accepted and cavitation attack reduced by the selection of more resistant materials. One very important factor in setting the correct $NPSH_A$ is the relative elevation of the pump and the vessel, from which the liquid is being pumped. Fluid friction in the suction line must also be taken into account, and the suction piping is usually a size bigger than the discharge piping.

5. Control of Flow-Enhanced Film Dissolution Attack

The control of this type of "chemical" erosion–corrosion of carbon–steel pipes in power plants may involve one or more of the following [51]:

Control of the water chemistry: pH and dissolved oxygen concentration.

Materials selection: replacement of carbon steel by, low-alloy chromium $>0.1\%$, low alloy chromium–molybdenum, 304 ss, and in very severe conditions Inconel, or by duplex piping with a thin inner layer of stainless steel or other high alloy.

Weld overlay: for protection and repair.

Flame spraying: minimum pipe diameter 600 mm.

Modification of operating conditions: temperature and quality, where wet steam is involved, and flow rate.

Changing the local geometry: for example, installing a larger control valve to reduce downstream turbulence.

In general, orifice plates and control valves should be kept well clear, at least 10 pipe diameters upstream of bends, to avoid excessive turbulence and erosion–corrosion at the latter.

The extensive and well-documented EPRI [51] report contains information regarding the detection and control of the problem.

6. Predictive Modeling

The application of computational fluid dynamics (CFD) to the problem of erosion–corrosion in single and multiphase flow systems, under conditions of disturbed flow, can help to quantify the effects of the system geometry on rates of erosion–corrosion leading to design improvements. The flow field, including flow separation recirculation and reattachment, and rates of mass transfer can be predicted for a wide range of system geometries [15, 71–75]. In addition, the velocities and angles of impact of suspended solid particles with the flow system walls can be determined for application to the calculation of the erosion rate [76–78]. Computer modeling has been applied to the prediction of wear in slurry pumps [79]. Such predictive modeling is in its infancy but substantial progress should be possible in the near future as our understanding of erosion–corrosion processes advances accompanied by ever-increasing computing power.

H. REFERENCES

1. ASTM G 15–97, "Standard Terminology Relating to Corrosion and Corrosion Testing," Annual Book of ASTM Standards, Vol. 03.02: Wear and Erosion: Metal Corrosion, West Conshohocken, PA, 1997, pp. 65–68.

2. U. Lotz, "Velocity Effects in Flow Induced Corrosion," in Proceedings of Symposium on Flow-Induced Corrosion; Fundamental Studies and Industry Experience, K. H. Kennelley, R. H. Hausler, and D. C. Silverman (Eds.), NACE, Houston, TX, 1991, pp. 8:1–8:22.
3. J. Weisman, "Two-Phase Flow Patterns," in Handbook of Fluids in Motion, N. P. Cheremisinoff, and R. Gupta (Eds.), Ann Arbor Science Publishers, Ann Arbor MI, 1983, pp. 409–424.
4. G. W. Govier and K. Aziz, The Flow of Complex Mixtures in Pipes, Van Nostrand Reinhold Company, New York, 1972, pp. 324, 326, 506.
5. API (American Petroleum Institute), Corrosion of Oil and Gas-Well Equipment, Book 2 of the Vocational Training Series, 2nd ed., Washington, DC, 1990, p. 8.
6. C. J. Houghton and R. V. Westermark, Mater. Perf., **22**(1), 16 (1983).
7. J. S. Smart III, "A Review of Erosion Corrosion in Oil and Gas Production," in Proceedings of Symposium on Flow-Induced Corrosion; Fundamental Studies and Industry Experience, K. H. Kennelley, R. H. Hausler, and D. C. Silverman (Eds.), NACE, Houston, TX, 1991, pp. 18:1–18:18.
8. W. Blatt, T. Kohley, U. Lotz, and E. Heitz, Corrosion, **45**, 793 (1989).
9. U. Lotz and J. Postlethwaite, Corros. Sci., **30**, 95 (1990).
10. G. Bianchi, G. Fiori., P. Longhi, and F. Mazza, Corrosion **34**, 396 (1978).
11. G. Schmitt, W. Bücken, and R. Fanebust, "Modeling Micro-Turbulences at Surface Imperfections as Related to Flow-induced Localized Corrosion and Its Prevention," Corrosion'91, Paper No. 465 NACE, Houston TX, 1991.
12. J. Postlethwaite, M. H. Dobbin, and K. Bergevin, Corrosion, **42**, 514 (1986).
13. F. P. Berger and K.-F., F.-L. Hau, Int. J. Heat Mass Transfer, **20**, 1185 (1977).
14. T. Sydberger and U. Lotz, J. Electrochem. Soc., **129**, 276 (1982).
15. S. Nesic, G. Adamopoulos, J. Postlethwaite, and D. J. Bergstrom, Can. J. Chem. Eng., **71**, 28 (1993).
16. Y. Wang and J. Postlethwaite, Corros. Sci., **39**, 1265 (1997).
17. J. Postlethwaite and U. Lotz, Can. J. Chem. Eng., **66**, 75 (1988).
18. E. Heitz, "Chemo-Mechanical Effects of Flow on Corrosion," in Proceedings of Symposium on Flow-Induced Corrosion; Fundamental Studies and Industry Experience, K. H. Kennelley, R. H. Hausler, and D. C. Silverman (Eds.), NACE, Houston, TX, 1991, pp. 1:1–1:29.
19. B. S. Poulson, "Erosion Corrosion," in Corrosion, 3rd ed., L. L. Shreir, R. A. Jarman, and G. T. Burstein (Eds.), Butterworth-Heinemann, Oxford, UK, 1994, pp. 1:293–1:303.
20. B. C. Syrett, Corrosion, **32**, 242 (1976).
21. E. F. C. Somerscales and H. Sanatgar, Bri. Corros. J., **27**, 36 (1992).
22. J. Postlethwaite, Y. Wang, G. Adamopoulos, and S. Nesic, "Relationship Between Modelled Turbulence Parameters and Corrosion Product Film Stability in Disturbed Single-Phase Aqueous Flow," in K. R. Trethaway and P. R. Roberge (Eds.), Modelling Aqueous Corrosion, Kluwer Academic Publishers, Dordrecht, The Netherlands, 1994, pp. 297–316.
23. R. H. Perry and D. Green (Eds.), Perry's Chemical Engineers' Handbook, 7th ed., McGraw-Hill, New York, 1997, p. 6:10.
24. V. L. Streeter, E. B. Wylie, and K. W. Bedford, Fluid Mechanics, 9th ed., McGraw-Hill, New York, 1998, pp. 105, 291.
25. C. O. Bennett and J. E. Myers, Momentum Heat and Mass Transfer, McGraw-Hill, New York, 1982, p. 168.
26. K. D. Efird, Corrosion, **33**, 3 (1977).
27. ASM, "Corrosion of Copper and Copper Alloys," in ASM Metals Handbook, Vol. 13, Corrosion, ASM Metals Park, OH, 1987, p. 624.
28. J. Kim, Phys. Fluids, **28**, 52 (1985).
29. J. L. Dawson and C. C. Shih, "Corrosion Under Flowing Conditions—An Overview and Model," in Proceedings of Symposium on Flow-Induced Corrosion; Fundamental Studies and Industry Experience, K. H. Kennelley, R. H. Hausler, and D. C. Silverman (Eds.), NACE, Houston, TX, 1991, pp. 2:1–2:12.
30. G. J. Danek, Jr., Naval Eng. J., **78**, 763 (1966).
31. G. Butler and E. G. Stroud, J. Appl. Chem., **15**, 325 (1965).
32. A. Cohen, Mater. Perfor., **32**, 56 (1993).

33. E. D. D. During, comp., Corrosion Atlas: A Collection of Illustrated Case Histories, Vol. 1: Carbon Steels; Vol. 2: Stainless Steels and Non-ferrous Materials: "Erosion-Corrosion of Copper Tubing," 06.05.34.01; "Valve Erosion," 04.01.32.01; "Pump Cavitation," 04.11.33.01; Elsevier, Amsterdam, The Netherlands, 1988.
34. J. Postlethwaite, B. J. Brady, M. W. Hawrylak, and E. B. Tinker, Corrosion, **34**, 245 (1978).
35. E. J. Wasp, J. P. Kenny, and R. L. Gandhi, "Solid-Liquid Flow: Slurry Pipeline Transportation," in Series on Bulk Materials Handling, Vol. 1 (1975/77) No. 4, Trans. Tech.: Publications, Clausthal, Germany, 1977, p. 144.
36. S. Nesic, "Erosion-Corrosion in Disturbed Flow," Ph.D. Thesis, University of Saskatchewan, Canada (1991).
37. J. Postlethwaite and S. Nesic, Corrosion, **49**, 850 (1993).
38. W. Madsen and R. Blickensderfer, "A New Flow-Through Slurry Erosion Wear Test," in J. E. Miller, F. E. Schmidt, Jr. (Eds.), Slurry Erosion: Uses Applications and Test Methods, ASTM STP 946, ASTM, West Conshohocken, PA, 1987, pp. 169–184.
39. P. J. Baker and B. E. A. Jacobs, A Guide to Slurry Pipeline Systems, BHRA Fluid Engineering, Cranfield, UK, 1979, p. 15.
40. E. Heitz, S. Weber, and R. Liebe, "Erosion Corrosion and Erosion of Various Materials in High Velocity Flows Containing Particles," in Proceedings of Symposium on Flow-Induced Corrosion; Fundamental Studies and Industry Experience, K. H. Kennelley, R. H. Hausler, and D. C. Silverman (Eds.), NACE, Houston, TX, 1991, pp. 5:1–5:15.
41. F. J. Heymann, "Liquid Impingement Erosion," in ASM Metals Handbook, Vol. 18, Friction, Wear and Lubrication Technology, ASM Metals Park, OH, 1992, pp. 221–232.
42. F. J. Heymann, Machine Design, Dec., 118 (1970).
43. Century Brass, The Century Heat Exchanger Tube Manual, Century Brass Products, Waterbury, CT, 1977.
44. C. M. Hansson and L. H. Hansson, "Cavitation Corrosion," in ASM Metals Handbook, Vol. 18, Friction, Wear and Lubrication Technology, ASM Metals Park, OH, 1992, pp. 214–220.
45. B. Angell, "Cavitation Damage," in Corrosion, 3rd ed., L. L. Shreir, R. A. Jarman, and G. T. Burstein (Eds.), Butterworth-Heinemann, Oxford, UK, 1994, pp. 8:197–8:207.
46. C. M. Preece, "Cavitation Erosion," in Treatise on Materials Science and Technology, C. M. Preece (Ed.), Vol. 16: Erosion, Academic, London, UK, 1979, pp. 253, 259, 261, 294.
47. D. McIntyre (Ed.), Forms of Corrosion, Recognition and Prevention, NACE Handbook 1, Houston, TX, Vol. 2, 1997, pp. 89, 93.
48. W. Glaeser, "Erosion–Corrosion Cavitation and Fretting," in Ref. 52, p. 72.
49. P. Griffith, J. Petroleum Technol., March, 361 (1984).
50. F. Giralt and O. Trass, Can. J. Chem. Eng, **54**, 148 (1976).
51. EPRI (Electric Power Research Institute), Flow Accelerated Corrosion in Power Plants, TR-106611, Pleasant Hill, CA, 1996, pp. 4:2, 6:25.
52. C. P. Dillon (Ed.), NACE Handbook 1, Forms of Corrosion, Recognition and Prevention, NACE, Houston, TX, 1982.
53. ASTM B 828, "Standard Practice for Making Capillary Joints by Soldering of Copper and Copper Alloy Tube and Fittings," Vol. 02.01: Copper and Copper Alloys, ASTM, West Conshohocken, PA, 1998.
54. M. G. Fontana, Corrosion Engineering, 3rd ed., McGraw-Hill, New York, 1986, p. 95.
55. W. Currer and J. S. Gerrard, "Practical Applications of Cathodic Protection," in Corrosion, 3rd ed., L. L. Shreir, R. A. Jarman, and G. T. Burstein (Eds.), Butterworth-Heinemann, Oxford, UK, 1994, p. 10 : 112.
56. B. W. Madsen, "Corrosive Wear," in ASM Metals Handbook, Vol. 18, Friction, Wear and Lubrication Technology, ASM Metals Park, OH, 1992, pp. 271–279.
57. J. Postlethwaite, Mater. Perfor., **26**(12), 41 (1987).
58. J. Postlethwaite, Corrosion, **35**, 475 (1979).
59. J. Postlethwaite, Corrosion, **37**, 1 (1981).
60. D. R. Bomberger, Mater. Prot., **4**, Sept., 43–49 (1965).
61. V. S. Sastri and M. Malaiyandi, Can. Metal., Q., **22**, 241 (1983).
62. R. D. Coale, T. L. Thompson, and R. P. Ehrlich, Trans. SME, AIME, **260**, Dec., 289 (1976).

63. M. E. Jennings, Mining Eng., Feb., 178 (1981).
64. A. G. Ostroff, Introduction to Oilfield Water Technology, NACE, Houston, TX, 1979, p. 293.
65. J. Postlethwaite, E. B. Tinker, and M. W. Hawrylak, Corrosion, **30**, 285 (1974).
66. R. W. Schutz and D. E. Thomas, "Corrosion of Titanium and Titanium Alloys," in Metals Handbook, 9th ed., Vol. 13, ASM, 1987, pp. 669–706, p. 696.
67. J. H. Tylczak, "Abrasive Wear," in ASM Metals Handbook, Vol. 18, Friction, Wear and Lubrication Technology, ASM Metals Park, OH, 1992, p. 189.
68. J. Dodd, "High-chromium Cast Irons," in Corrosion, 3rd ed., L. L. Shreir, R. A. Jarman, and G. T. Burstein (Eds.), Butterworth-Heinemann, Oxford, UK, 1994, pp. 3 : 128–3 : 137.
69. G. Wilson, "The Design Aspects of Centrifugal Pumps for Abrasive Slurries," in Proceedings of the 2nd International Conference on Hydraulic Transport of Solids in Pipes, BHRA Fluid Engineering, Cranfield, U.K., 1972, pp. H2:25–H2:52.
70. J. Tullis, Hydraulics of Pipelines: Pumps, Valves, Cavitation, Transients, Wiley, New York, 1989, pp. 59, 78.
71. S. Nesic and J. Postlethwaite, Corrosion, **46**, 874 (1990).
72. S. Nesic and J. Postlethwaite, Can. J. Chem. Eng., **69**, 698 (1991).
73. S. Nesic, J. Postlethwaite, and D. J. Bergstrom, Int. J. Heat Mass Transfer, **35**, 1977 (1992).
74. J. Postlethwaite, S. Nesic, and G. Adamopoulos, Mater. Sci. Forum, **111–112**, 53 (1992).
75. J. Postlethwaite, S. Nesic, G. Adamopoulos, and D. J. Bergstrom, Corrosion Sci., **35**, 627 (1993).
76. S. Nesic and J. Postlethwaite, Can. J. Chem. Eng., **69**, 704 (1991).
77. S. Nesic and J. Postlethwaite, Corrosion, **47**, 582 (1991).
78. H. Zeisel and F. Durst, "Computations of Erosion–Corrosion Processes in Separated Two-Phase Flows," in Proceedings of Symposium on Flow-Induced Corrosion; Fundamental Studies and Industry Experience, K. H. Kennelley, R. H. Hausler, and D. C. Silverman (Eds.), NACE, Houston, TX, 1991, pp. 9:1–9:21.
79. M. C. Roco, Corrosion, **46**, 424 (1990).